J MATER SCI **41** (2006) 2627–2630

Fabrication of a nano-magnet on a piezo-driven tip in a TEM sample holder

M. TAKEGUCHI*
High Voltage Electron Microscopy Station, National Institute for Materials Science, 3-13 Sakura, Tsukuba, 305-0003, Japan
E-mail: takeguchi.masaki@nims.go.jp

M. SHIMOJO
High Voltage Electron Microscopy Station, National Institute for Materials Science, 3-13 Sakura, Tsukuba, 305-0003, Japan; Advanced Science Research Laboratory, Saitama Institute of Technology, 1690 Fusaiji, Okabe-machi, Saitama, 369-0293, Japan

R. CHE, K. FURUYA
High Voltage Electron Microscopy Station, National Institute for Materials Science, 3-13 Sakura, Tsukuba, 305-0003, Japan

Published online: 17 April 2006

A nanometer-sized magnet (nano-magnet) was fabricated on the tip of a tungsten needle by electron-beam-induced deposition with $Fe(CO)_5$ gas. The needle tip, which can be moved with a stepping motor and piezo-driver, was attached inside a specially designed TEM specimen holder. This nano-magnet on the piezo-driven tip is capable of making an approach to magnetic nanostructures formed on a substrate so that the nanometer-scale magnetic interaction could be studied. Electron holography observation of the magnetic field around the nano-magnet showed that the residual magnetic flux density B_r of the nano-magnet was about 0.48 T.

1. Introduction

Nanometer-sized ferromagnetic structures have attracted much attention because of their interesting properties and their potential practical application to advanced submicron magnetic devices. An understanding of the switching behavior of the magnetic nanostructures has been a significant issue from the point of view of application to high-density magnetic recording and magnetic random access memory. Properties of magnetic nanostructures strongly depend on their shape and size [1]. Their spatial distribution is also important because a magnetic interaction between densely packed nanometer-sized magnetic elements such as rings and dots via magnetostatic stray fields influences the switching behavior [2]. Therefore, recently, great effort to fabricate magnetic nanostructures with the desired shape at the desired position has been made [3, 4], and the magnetic interaction between the nanostructures and macroscopic external magnetic fields has been investigated [5, 6]. However, characterization of magnetic properties of individual nanostructures and a nanostructure-nanostructure magnetic interaction is rare.

Transmission electron microscopes (TEM) equipped with a specially designed sample holder, including a needle tip driven by piezo devices, have been widely employed to observe nanometer-scale mechanical and physical interactions between the tip and the sample. For instance, *in situ* atomic-level observation of deformation processes [7], quantum nano-wiring [8], cracking processes [9], etc. has been reported so far. Electron holography, which can be performed inside the TEM, has enabled us to observe electric and magnetic fields between the tip and the sample [10, 11]. This combination of electron holography and a piezo-tip sample holder is capable of observatingvthe magnetic interaction between magnetic nanostructures.

*Author to whom all correspondence should be addressed.
0022-2461
DOI: 10.1007/s10853-006-7825-8

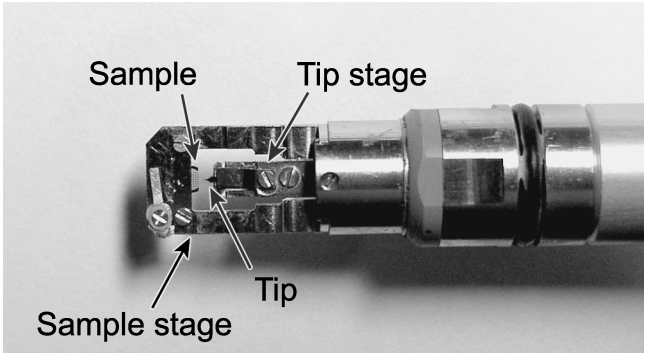

Figure 1 Head part of a specially designed TEM sample holder. A tip stage, which is built-in inside the holder body, can be moved with a stepping motor (for rough approach) and a piezo-driver (for three-axes fine positioning). Samples, on an edge of which magnetic nanostructures are fabricated by EBID, are mounted on a sample stage supported on the holder body.

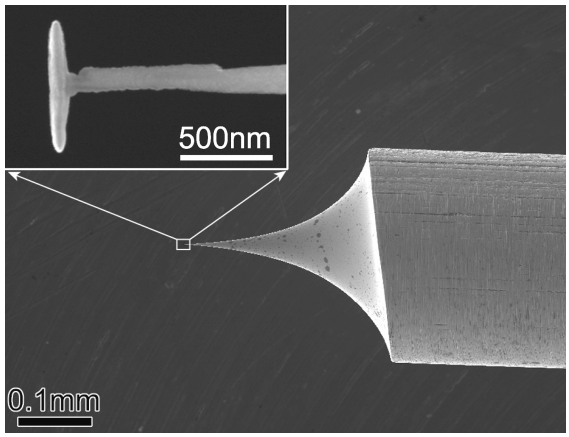

Figure 2 Scanning electron micrograph of the tungsten tip with a nano-magnet. The inset shows an enlargement of the nano-magnet part.

In the present paper, a nanometer-sized magnet (nano-magnet) is formed on the apex of a tungsten needle tip by focused electron-beam-induced deposition (EBID) with iron carbonyl, $Fe(CO)_5$. EBID is one of the most promising methods for size and position controllable fabrication. In this process, metal-organic gases are decomposed by the electron beam, resulting in metal deposition at the desired position, which can be controlled by the position of the beam [12–21]. The tip is set on a stage, which can be moved with a stepping motor and a piezo-driver, and a substrate, on which various shaped magnetic nanostructures are fabricated by EBID. This assembly is mounted on a sample stage in a specially designed TEM sample holder, so that the magnetic interaction could be observed by approaching the nano-magnet to the magnetic nanostructures. The remanent magnetic behavior of the nano-magnet is evaluated by measuring the residual magnetic flux density B_r using off-axis electron holography.

2. Experiments

Fig. 1 shows the head part of a specially designed TEM sample holder for a JEOL JEM-3000F 300-keV field-emission-gun transmission electron microscope equipped with an electron biprism. The tip stage, which is built-in inside the holder body, can be moved with a stepping motor (for rough approach) and a piezo-driver (for three-axes fine positioning). The point of the tungsten tip was electrochemically etched to make it sharper than 150 nm, and then a 20-nm thick layer of gold was deposited on the surface of the tip to avoid charging. Samples used in the present work were Si thin films or Cu grids, on which magnetic nanostructures were fabricated by EBID as described later. These samples were mounted on the sample stage supported on the holder body.

Fig. 2 shows a scanning electron micrograph of the tungsten tip with a nanometer-sized magnet (nano-magnet). The insert shows an enlargement of the nano-magnet, which was fabricated perpendicular to the tip axis by EBID with iron carbonyl, $Fe(CO)_5$. Its width and length were 120 nm and 700 nm, respectively.

EBID was carried out using a JEOL JSM-7800FV 30-kV field-emission-gun scanning electron microscope at room temperature. The beam position was controlled by an external deflector voltage input using a computer with digital-analog converters. Carbonyl gases were introduced into the specimen chamber through a nozzle with an inner diameter of about 0.2 mm, which was connected with a gas source reservoir through a gas pipe line and a leak valve. The nozzle tip was about 1 mm from the electron beam position. The partial pressure of the gas was controlled to be about 7×10^{-5} Pa using the leak valve. The electron beam current was about 0.8 nA with a beam diameter of 4 nm. The details of the gas introduction system and EBID method have been described elsewhere [18].

The magnetic performance of the nano-magnet was characterized by electron holography. The electron wave passing through the sample and vacuum regions is deflected by the electrostatic potential around the biprism so that an interference pattern is formed in the image plane. This interference pattern is called an "electron hologram", in which phase information of the object passing through the sample can be recorded. By reconstructing the hologram, the phase shift due to electric and/or magnetic fields is extracted quantitatively. The objective lens was turned off during the electron holography experiment. At that time, the residual magnetic field at the sample position is estimated to be less than 100 mT. A minilens located below the objective lens was used so that off-axis holograms were formed on a Gatan Ultrascan CCD camera integrated in the Gatan imaging filter.

3. Results and discussion

Fig. 3 shows a TEM image indicating a typical experimental state, in which the tungsten tip with the nano-magnet

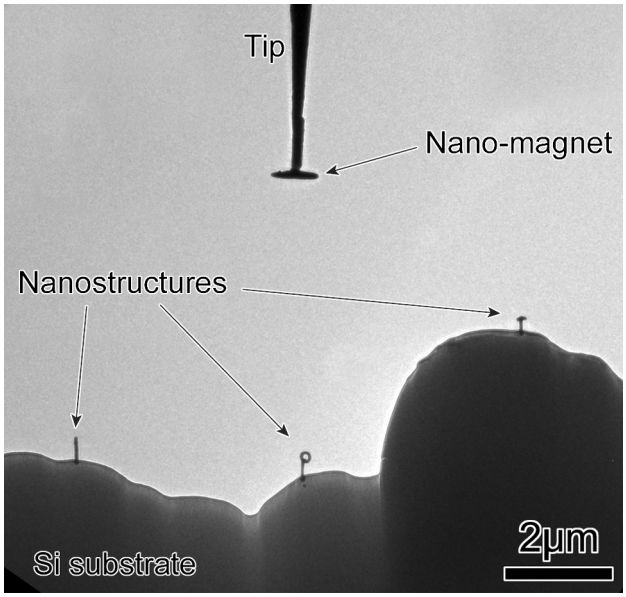

Figure 3 TEM image the tungsten tip with a nano-magnet and some nanostructures with various shapes (e.g., nano-rod, nano-rod with a ring head and nano-rod with a bar head) on a Si sample edge.

and some nanostructures with various shapes (e.g., nano-rod, nano-rod with a ring head and nano-rod with a bar head) on a Si sample edge are seen. The tip was positioned by the XY piezo-drivers. The Z-height of the tip was aligned to that of the sample so that both the tip and the sample were in focus.

The remnant magnetic field of the nano-magnet was evaluated by measuring the residual magnetic flux density B_r by off-axis electron holography. Fig. 4a shows an electron hologram of the nano-magnet. The phase image was obtained by digital reconstruction as described in the literature [18]. The phase shift $\Delta\varphi$ of the electron wave passing through a magnetic sample is expressed by

$$\Delta\varphi = C_E \int V_0(x, y)\,\mathrm{d}z - 2\pi \frac{e}{h} \iint B_\perp(x, y)dxdz \tag{1}$$

where x is a direction in the plane of the sample, z is the electron beam direction, C_E is an energy-dependent constant (0.00728 rad V^{-1} nm^{-1} at 200 kV), V_o is the mean inner potential, and$B_\perp$ is the component of magnetic flux density perpendicular to x and z. The phase of the electron wave passing through the nano-magnet is modulated by the internal magnetic field and the external magnetic stray field around the nano-magnet in addition to the mean inner potential of the nano-magnet as shown in Fig. 5. The phase change due to the internal magnetic field is described as

$$\Delta\varphi = 2\pi \frac{e}{h} BS \tag{2}$$

Fig. 4b shows the phase image reconstructed from Fig. 4a, with an amplification factor of 4. The spacing of the dark line corresponds to a phase shift of $\pi/2$. A TEM image of the nano-magnet was superimposed in this figure. A line profile of the phase distribution across the line in Fig. 4b is indicated in Fig. 4c. Since interference fringes in the nano-magnet were overlaid on the nano-magnet contrast, phase information at the position of the nano-magnet could not be successfully extracted. The phase jump across the nano-magnet was measured to be about 12.2 rad. However, as mentioned above, this phase jump was caused by the sum of the phase shift due to the internal magnetic field and the vertical integration of the external magnetic field at the nano-magnet position. The phase change due to the external magnetic field at the nano-magnet position was extrapolated approximately from the phase inclination near the nano-magnet, and found to be 2.9 rad. Therefore, the phase shift due to the internal magnetic field was estimated to be about 15.1 rad, which corresponds to the magnetic flux of 9.86×10^{-15} Wb.

The shape of the cross-section of the nano-magnet can be assumed to be elliptic. The thickness of the nano-magnet was estimated using an amplitude image obtained from Fig. 4a and a reference hologram, taken from the same field of view without the sample. The relative thick-

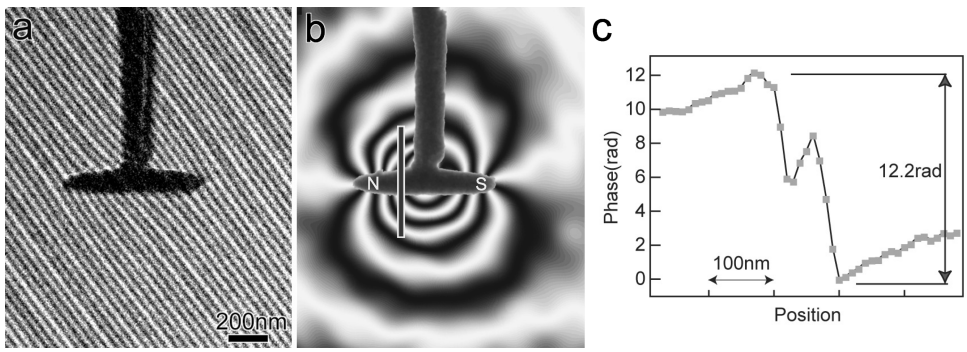

Figure 4 (a) Electron hologram of a nano-magnet. (b) Reconstructed phase image with an amplification factor of 4. (c) The line profile of the phase distribution across a line in Fig. 4b.

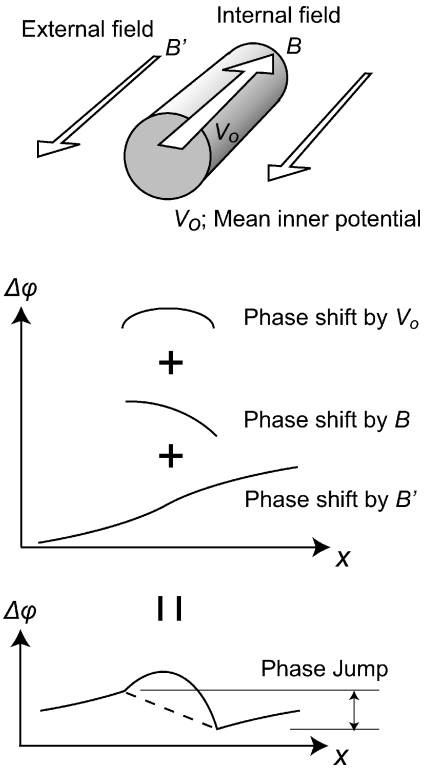

Figure 5 Schematic drawing of the electron wave after passing through a nano-magnet modulated by the internal and external magnetic fields in addition to the mean inner potential.

ness of the sample can be estimated from the expression

$$\frac{t}{\lambda_i} = -2\ln(Amp_n) \tag{3}$$

where t is the thickness, λ_i is the bulk inelastic mean free path, and Amp_n represents the amplitude image as normalized by the amplitude image of a reference hologram acquired under identical illumination conditions [19]. Assuming that the inelastic mean free path of this sample is identical to that of iron ($\lambda_i = 96$ at 200 kV), the thickness of the center of the line in Fig. 4b was estimated to be about 220 nm. The nano-magnet width was about 120 nm. Thus, the elliptical-shape cross-section of the nano-magnet at the position of the line in Fig. 4b was about 2.07×10^{-14} m^{-2}, and therefore the residual magnetic flux density B_r was calculated to be about 0.48 T.

Hence, it was found that the as-formed nano-magnet has a considerable B_r value, which would be sufficient to interact with nanostructures of various shapes on the substrate. Experiment on magnetic interactions between nano-magnets and nanostructures are currently in progress.

4. Conclusions

A special TEM sample holder for *in situ* experiment to measure a magnetic interaction between a nano-magnet and various shaped magnetic nanostructures was developed. The nano-magnet was fabricated on a tungsten needle tip by EBID with $Fe(CO)_5$ gas. The needle tip set in the TEM sample holder body can be moved with a stepping motor and piezo-driver so that the nano-magnet could approach the magnetic nanostructures formed on a substrate. Electron holography observation of the magnetic field around the nano-magnet showed that the residual magnetic flux density B_r of the nano-magnet was about 0.48 T, which is sufficient to interact with the magnetic nanostructures.

References

1. D. J. SMITH, R. E. DUNIN-BORKOWSKI, M. R. MCCARTNEY, B. KARDYNAL and M. R. SCHEINFEIN, *J. Appl. Phys.* **87** (2000) 7400.
2. U. WELP, V. K. VLASKO-VLASOV, G. W. CRABTREE, J. HILLER and N. ZALUZEC, *ibid.* **93** (2003) 7056.
3. S. P. LI, M. NATALI, A. LEBIB, A. PEPIN, Y. CHEN and Y. B. XU, *J. Magn. Magn. Mater.* **241** (2002) 447.
4. Y. OTANI, B. PANNETIER, J. P. NOZIERES and D. GIVORD, *ibid.* **126** (1993) 622.
5. A. SUGAWARA, T. COYLE, G. G. HEMBREE and M. R. SCHEINFEIN, *Appl. Phys. Lett.* **70** (1997) 1043.
6. K. LIU, J. NOGUES, C. LEIGHTON, H. MASUDA, K. NISHIO, I. V. ROSHCHIN and I. K. SCHULLER, *ibid.* 81 (2002) 4434.
7. T. KIZUKA, H. OHMI, T. SUMI, K. KUMAZAWA, S. DEGUCHI, M. NARUSE, S. FUJISAWA, S. SASAKI, A. YABE and Y. ENOMOTO, *Jpn. J. Appl. Phys.* **40** (2001) L170.
8. H. OHNISHI, Y. KONDO and K. TAKAYANAGI, *Nature* **395** (1998) 780.
9. K. MATSUNAGA, S. II, C. IWAMOTO, T. YAMAMOTO and Y. IKUHARA, *Nanotechnology* **15** (2004) S376.
10. D. SHINDO, Y. PARK, Y. GAO and H. S. PARK, *J. Appl. Phys.* **95** (2004) 6521.
11. J. CUMINGS, A. ZETTL, M. R. MCCARTNEY and J. C. H. SPENCE, *Phys. Rev. Lett.* **88** (2002) 056804-1.
12. H. W. P. KOOPS, A. KAYA and J. J. WEBER, *Vac. Sci. Technol. B* **13** (1995) 2400.
13. H. W. P. KOOPS, C. SCHOSSLER, A. KAYA and M. J. WEBER, *ibid.* **14** (1996) 4105.
14. I. UTKE, P. HOFFMANN, B. DWIR, K. LEIFER, E. KAPON and P. J. DOPPELT, *J. Vac. Sci. Technol. B* **18** (2000) 3168.
15. I. UTKE, A. LUISIER, P. HOFFMANN, D. LAUB and P. A. BUFFAR, *Appl. Phys. Lett.* **81** (2002) 3245.
16. K. MITSUISHI, M. SHIMOJO, M. HAN and K. FURUYA, *ibid.* **83** (2003) 2064.
17. M. TANAKA, M. SHIMOJO, K. MITSUISHI and K. FURUYA, *Appl. Phys. A* **78** (2004) 543.
18. M. SHIMOJO, K. MITSUISHI, A. TAMEIKE and K. FURUYA, *J. Vac. Sci. Technol. B* **22** (2004) 742.
19. M. HAN, K. MITSUISHI, M. SHIMOJO and K. FURUYA, *ibid.* **84** (2004) 1281.
20. R. R. KUNZ and T. M. MAYER, *Appl. Phys. Lett.* **50** (1987) 962.
21. M. SHIMOJO, M. TAKEGUCHI, M. TANAKA, K. MITSUISHI and K. FURUYA, *Appl. Phys. A* **79** (2004) 1869.
22. P. A. MIDGLEY, *Micron* **32** (2001) 167.
23. M. R. MCCARTNEY and M. GAJDARDZISKA-JOSIFOVSKA, *Ultramicroscopy* **53** (1994) 283.